Chapter 3

Monte Carlo Simulations of Nuclear Fuel Burnup

Raghava R. Kommalapati, Fiifi Asah-Opoku,
Hongbo Du and Ziaul Huque

Additional information is available at the end of the chapter

http://dx.doi.org/10.5772/62572

Abstract

In the operation of a nuclear power plant, it is very important to determine the time evolution of material composition and radionuclide inventory during the entire operation of the plant. In the experiments, the Monte Carlo N-Particle eXtended (MCNPX) code was found to be accurate in predicting the uranium fuel depletion, the plutonium production and the buildup of most of the fission products in a nuclear reactor. The goal in this chapter is to analyze the effect of different nuclear fuel grades on the total radioactivity of the reactor core by employing nuclear burnup calculations for the three different fuels: mixed oxide fuel (MOX), uranium oxide fuel (UOX) and commercially enriched uranium (CEU), utilizing simulations with MCNPX code. The calculated results indicate that there is a buildup of plutonium isotopes for UOX and CEU, whereas there is a decline in the plutonium radioisotopes for MOX fuel with burnup time. The study of reactor neutronic parameters showed UOX fuel performs better relative to MOX and CEU. Zircaloy, with low thermal neutron absorption cross-section and high thermal conductivity, produced better results for the effective multiplication factor K_{eff} and hence proved to be a much more effective clad material.

Keywords: nuclear fuel, MCNPX code, burnup, radionuclide inventory, fuel burnup

1. Introduction

Use of nuclear energy as a sustainable energy supply has both good and harmful effects like every other natural resource. The issue is mostly with the spent nuclear material that is left after the energy extraction which is no longer efficient in the splitting of its atoms to produce energy. This residual material is known as spent nuclear fuel (SNF) and contains highly radioactive elements such as uranium and plutonium. In the operation of a nuclear power plant, it is important

to determine the time development of material composition and radionuclide inventory during the entire operation of the plant. The determination of plutonium (Pu) in environmental samples is also important for investigating radiotoxicity and the long-term radiation effects on humans that are attributed to Pu rather than the other transuranic elements [1]. The determination of the elemental and isotopic compositions of Pu in spent nuclear fuels is required for fuel characterization [2], and also the management of radioactive waste [3]. According to the U.S Nuclear Regulatory Commission, the elements contained in high-level waste include plutonium-239 (half-life: 24,000 years) and plutonium-240 (half-life: 6800 years). The content of Pu isotopes in high burnup spent nuclear fuel samples (33.21–59.03 GWd/MtU) were determined by alpha and mass spectrometry [4]. While it may be necessary to determine Pu content in spent fuel due to the extremely long half-life of Pu, it is also important to quantify spent fuel based on the total concentrations of key actinides and non-actinides to estimate the entire radioactive hazard posed by these fuels.

Much research work has been done in the area of sustainable nuclear energy. Some research work on nuclear burnup calculations focused on the analysis of the accuracy of the Monte Carlo Nuclear Particle (MCNP) Code as compared to other computer codes such as BUCCAL 1, GETERA Code and others. Accuracy of the new Monte Carlo based burnup computer code has been studied [5]. The research involved direct usage of neutron absorption tally generated by MCNP5 to determine new nuclide inventories. This eliminates the need to calculate neutron fluxes as input to other computer codes to generate the nuclide inventories and thus incorporates fully the capabilities of MCNP. Code-to-code comparison of BUCAL 1 with several burnup codes showed good agreement. The research shows the accuracy of the Monte Carlo Code in predicting the depletion and generation of radionuclide inventories. Monte Carlo burnup simulations of isotope correlation experiments have also been determined using the NPP Obrigheim [6]. In the experiment, the Monte Carlo Nuclear Particle eXtended (MCNPX) code was found to be accurate in predicting the uranium fuel depletion, the plutonium production and the buildup of most of the fission products in a nuclear reactor. The direct integration of the cinder.dat file as the decay code for MCNPX makes it more accurate than in previous experiments when the MCNP transport code is simply linked to other codes such as ORIGEN.

The GETERA code [7] was used to calculate fuel burnup in a miniature neutron source reactor (MNSR). A list of 19 radionuclides, including 13 fission products and 6 actinides, was identified and the total radioactivity of the MNSR at the end of the reactor core life was calculated based on these nuclides. This was found to be 9.462×10^{13} Bq. This research used highly enriched uranium as fuel in the MNSR core and does not provide comparisons of the radiological hazards associated with other fuels. The results from the research indicated that the amount of 235U and 238U after burnup decreased about 13.669 and 0.065 g, respectively, thus predicting again the accuracy of the code in estimating the depletion of uranium.

The next section gives details on the Monte Carlo methods for simulating the fuel burnup in nuclear power plants in this research. The three different fuel grades, mixed oxide fuel (MOX), uranium oxide fuel (UOX) and commercially enriched uranium (CEU), would be used for the

http://dx.doi.org/10.5772/62572

fuel burnup simulations. Also, three different clad materials (zirconium, zircaloy and stainless steel) would be investigated based on their influence on the K_{eff}.

2. Methodology

2.1. Monte Carlo methods for nuclear plants

The principle behind the MCNP is statistical sampling, which makes use of the randomness of numbers. The MCNP records the trajectory of neutrons emitted by a source and determines whether the neutron is able to penetrate a shield after interacting with radioisotopes on the shield [8, 9]. The set-up for the simulation using MCNP5 in this study is made up of three main interacting packages of software obtained from the Radiation Safety Information and Computational Center of the Oak Ridge National Laboratory, Tennessee, USA. These three packages are MCNP1.05/MCNPX, CINDER 1.05 and MONTEBURNS 2.0.

The whole simulation process starts with an input data file to the MCNP5 as shown in **Figure 1**. Some of the parameters in the input data file include initial material compositions, geometry specifications (cell and surface cards), material specifications and source definition cards. Based on the output data required, MCNP produces a wide variety of output data files. Keys among these output files will be the group cross-sections and the neutron fluxes of materials. MONTEBURNS, which links MCNP5 and CINDER, transfers one group cross-section and neutron fluxes generated by MCNP to CINDER. This serves as the burnup or decay code for the set-up. CINDER processes these input files and generates output results such as burnup values and final material compositions. The resulting material compositions are transferred again to MCNP in a repeated or cyclic process. The end of a cycle repents the end of a burnup step. The next burnup step continues with the next cycle.

2.2. The MCNPX code

MCNPX is a software package popularly used to simulate various kinds of reactions pertaining to neutron, photon, electron transport and radioactive particles. This computer code package also has the capability of simulating nuclear burnup reactions and calculating the radionuclide inventory due to fission of fissile or fissionable isotopes and transmutation of parent nuclides. The code eliminates the need for the combination of the MCNP code with the nuclear burnup code ORIGEN or CINDER, in which one group cross-sections and fluxes are transferred from MCNP to the decay code ORIGEN or CINDER using monteburns. The MCNPX code has the CINDER.dat file responsible for nuclear fuel burnup as part of its buildup which allows the direct transfer of one-group reaction rates (cross-sections) and 63 group neutron fluxes to the depletion code cinder for decay calculations. In this study, the MCNPX is used to simulate nuclear fuel burnup calculations for a pressurized water reactor system using three different fuel grades: UOX, CEU and MOX.

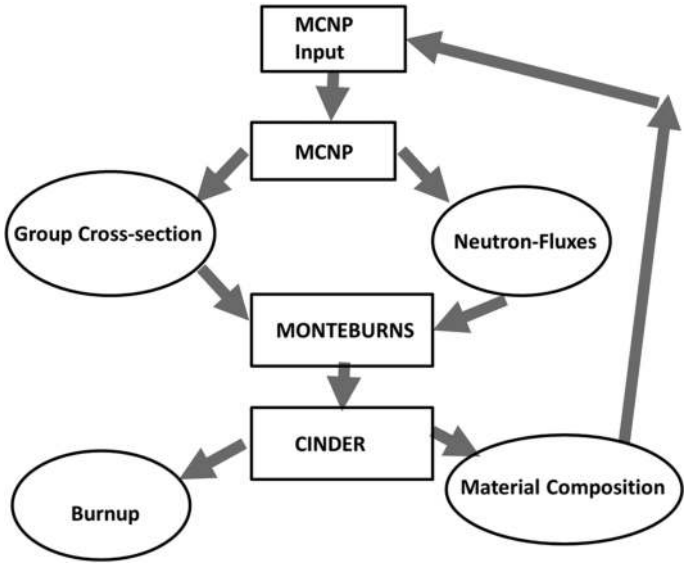

Figure 1. Simplified experimental model using MCNP and MONTEBURNS.

The inventory of important nuclides would then be analyzed with burnup time for each fuel. This would be done by burning the fuel in the reactor core for 220 days using a 30-day time step. A 10-day time step is allowed for core maintenance operations. The performance of each fuel grade on the effective multiplicative factor, reactivity and reactor core life would also be analyzed based on the inventory of radionuclides for each fuel grade. The three fuel grades would also be compared based on reactor neutronic parameters such as the reactivity and neutron fluxes. Finally, the total radioactivity of the reactor core would be analyzed using different fuel grades. This would be the key in estimating the radiological hazard at the end of the core life of the reactor.

2.3. The lattice cell structure

Nuclear reactor cores are constructed as either rectangular or hexagonal lattices of assemblies. The lattice structure could consist of several different shapes or identical shapes. The lattice assembly consists of the fuel, control and instrumentation pins surrounded by water or other material that moderates neutron energy and carries away the heat generated as a result of the fission process. The basic shapes which make up the lattice are known as unit cells or pin cells [10].

Various types of assemblies are then arranged in a lattice structure to form the reactor core. The two most common lattice structures used for nuclear reactor cores are the rectangular lattice, used in water cooled reactors, or a hexagonal lattice, more common in sodium-and-gas-cooled reactors. The lattice geometry is described by three main parameters: the unit cell shape;

http://dx.doi.org/10.5772/62572

the distance between the centers of adjacent unit cells, referred to as the lattice pitch; and the lattice dimension, which is a measure of how many units form the lattice.

The rectangular lattice for water-cooled reactors is used in this research. The lattice geometry is set up using the lattice fill matrix of the MCNPX visual editor. The total number of unit cells is hence NxNy. The lattice cell is shown below:

$$3\ 0\ 8\ -7\ 10\ -9\ \ U=1\ \text{lat}=1$$
$$\text{fill}=\ -24:24\ -24:24\ -0:0$$

The first number is the cell number, which is 3. The second number 0 is the material number indicating a void material. The next four numbers are the surface numbers of the planes which are the sides of the rectangular shape. The U card specifies the universe to which the cell belongs, which in this case is 1. A cell is filled with a universe which is either a lattice or an arbitrary collection of cells. There are 24 unit cells on either side of the center lattice element in the x and y direction as indicated by the fill card with no unit cells in the z direction. **Figure 2** shows the lattice geometry together with the cell and surface numbers as can be seen when using the MCNPX visual editor. This shows the position of cells and surfaces in the reactor core lattice and how they are related in the system geometry.

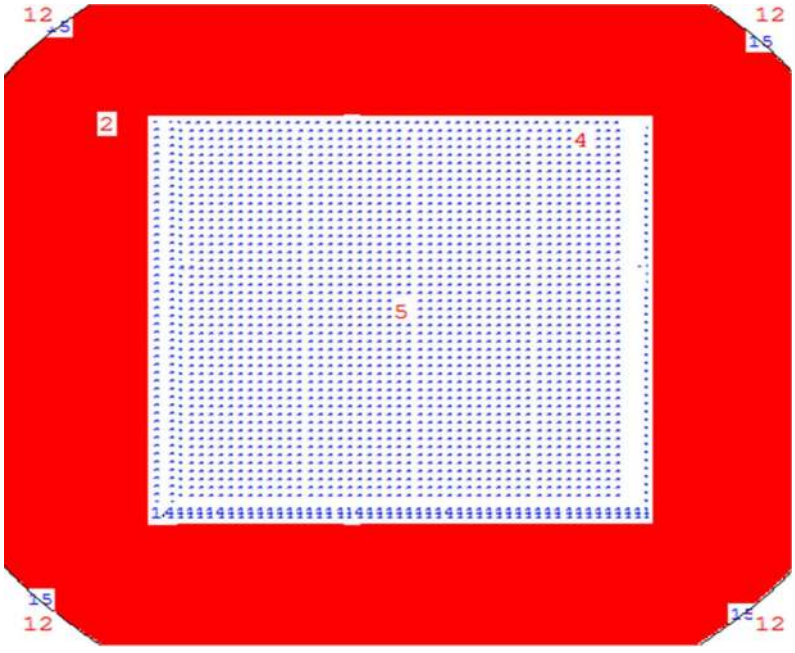

Figure 2. MCNPX simplified geometry showing both cell and surface numbers.

2.4. The critical reactor core system

A critical reactor system usually has an effective multiplication factor of 1. This usually means that the neutron production in one generation is equal to the neutron lost through either absorption or leakage in the preceding generation. While the sub-critical reactor might need an external neutron supply through accelerator-driven systems, the critical reactor system is self-sustaining. Usually, the size of the fuel cylinder and the density are much smaller for critical systems. The geometry of the critical pressurized water reactor system is modeled using the MCNPX visual editor. The material composition of the reactor core showing nuclide atom fractions for the three fuel grades and also for the clad material and moderator used is shown in **Table 1**.

Material name	Nuclide atom fraction
UO_2	^{16}O 5.85402 × 10^{-3}; ^{235}U 3.862438 × 10^{-2} ^{238}U 0.9555216
Commercially enriched uranium	^{234}U 3 × 10^{-4}; ^{235}U 2.96 × 10^{-2}; ^{238}U9.701 × 10^{-1}
Mixed oxide fuel	^{16}O 5.88402 × 10^{-3}; ^{235}U 2.5 × 10^{-3}; ^{238}U 0.9386; ^{238}Pu 1.1147 × 10^{-4}; ^{239}Pu 4.150 × 10^{-2}; ^{240}Pu 7.9657 × 10^{-4}; ^{241}Pu 1.001 × 10^{-2}; ^{242}Pu 5.6388 × 10^{-4}
Cladding (zirconium alloy)	^{50}Cr 9.98 × 10^{-4}; Fe 1.499 × 10^{-3}; Zr 0.982499; ^{112}Sn 0.014999
Moderator (light water)	^{1}H 4.7716 × 10^{-2}; ^{16}O 2.3858 × 10^{-2}; ^{10}B 3.6346 × 10^{-6}; ^{11}B 1.6226 × 10^{-5}

Table 1. Material composition of reactor core.

2.5. Normalization of tally plots

The tally plots are used to specify what needs to be investigated from the MCNP calculations. There are seven standard tallies available for use in MCNP. These tally cards are specified by Fn cards, where n specifies the tally number. SD cards are also used together with tally cards where necessary. The SD card is used to input a constant (a new area or volume) to divide the tally in cases where MCNP cannot calculate the area or volume for the regions. In all, three tally cards are used in this simulation. These are the f2, f4 and f7 tally cards. These were used to find out the flux across a surface, the track length in a cell and the track length estimate of fission energy deposition, respectively. The flux actually gives an idea of the flow of a physical property with time variation. The unit is given as quantity/(area × time). Some very important deductions were made from the flux calculations.

The tally bin width is usually normalized by dividing by the energy bin width. This gives a much broader representation of the particle distribution with energy. When a logarithmic scale is used for both axes, the visual representation is further obscured, with the tallies seen to decrease gradually with increasing energy or spread wide across the entire plot area. The two methods for normalizing energy-dependent tally are divided by the width of each energy bin or dividing by the logarithmic width of each energy bin [11].

http://dx.doi.org/10.5772/62572

The logarithmic width of the energy bin is referred to as the lethargy width. The governing equations are as follows (Eq. 1) [11]:

$$T_i = \int_{Elt}^{E_{ut}} f(E)dE \tag{1}$$

where $E_{ut}$and E_{lt} are the upper and lower energy bin width, and $f(E)$ is the flux or reaction rate. The tallies (T_i) tend to be small for small energy bins and large for large energy bins as can be seen from the above equation.

The normalized energy-dependent tally is calculated by dividing by the width of the energy bin and is shown below (Eq. 2):

$$I(E) = \frac{\int_{E_{lt}}^{Eut} f(E)dE}{\int_{E_{lt}}^{E_{ut}} dt} = \frac{T_i}{E_{ut} - E_{lt}} \text{ (tally units)/unit energy} \tag{2}$$

For lethargy normed tallies, a definition is required for lethargy. Neutron lethargy is defined in the analysis of nuclear reactors as the logarithmic energy loss of neutrons scattered elastically. Mathematically, this is defined as in Eq. 3:

$$U = \text{In}\frac{E_0}{E} = \text{In}(E_0 - E) \tag{3}$$

where U is the neutron lethargy.

The difference in the log of the energy bins is related to the neutron lethargy as follows (Eq. 4):

$$\text{In}(E_{ut}) - \text{In}(E_{lt}) = U_{lt} - U_{ut} \tag{4}$$

where U_{lt} is the lethargy at E_{lt} and U_{ut} is the lethargy at E_{ut}. The lethargy normed value (FI) is then given by the relation (Eq. 5):

$$F_i(U) = \frac{T_i}{\text{In}(E_{ut} - E_{lt})} = \frac{T_i}{U_{lt} - U_{ut}} \text{(tally units)/(unit lethargy)} \tag{5}$$

2.6. Setting up a criticality problem

The criticality calculation generally gives an idea about the ability of the reactor core to maintain a self-sustaining nuclear chain reaction. This is represented by the value of the effective multiplication factor, K_{eff}. For reactors, which are infinitely large, an infinite multi-

plication factor represents the criticality because it assumes that no neutrons leak out of the reactor. For a complete description of the life cycle of a real finite reactor, it is necessary to account for the neutrons that leak out. The effective multiplication factor takes this into account. Mathematically, K_{eff} is defined as follows (Eq. 6):

$$K_{eff} = \frac{\text{neutron production from fission in one generation}}{\text{neutron absorbed} + \text{neutron leakage in preceding generation}} \quad (6)$$

The calculation of K_{eff} consists of estimating the mean number of fission neutrons produced in one generation per fission neutron started. The K_{eff} cycle is thus the computational equivalent of a fission generation, where a cycle is used to denote the computed estimate of an actual fission generation. MCNPX uses three different estimates to set up K_{eff} (absorption, collision and track length) estimate. The final result is the statistically combined result for the three estimates.

The KCODE card is used together with a number of cards to set up a criticality problem. These cards specify the initial spatial distribution of fission points and include the KSRC card, SDEF card and SRCTP card. The KSRC card sets the initial x, y, z locations of fission points. The SDEF card is used to define points uniformly in volume whilst the SRCTP card is defined from a previous MCNPX criticality calculation. A typical KCODE card used together with a KSRC card has the following format:

KCODE: 10000 1.000000 70 150 KSRC: 0.0000 0.0000 0.0000

The card above indicates that the nominal number of source histories is 10000 with the initial K_{eff} guess kept as 1.00. The number of inactive cycles skipped before active K_{eff} accumulation is 70 and the total number of cycles that run in the problem is 150. The KSRC card indicates that the x, y, z locations for initial fission source points were taken from the origin. The criticality calculations were performed with help from Bunde Kermit at the U.S Department of Energy.

In this research, different fuel grades and different cladding materials were used for the same reactor core configuration to investigate the effect of these on the criticality. The different fuel grades used were MOX, UOX and CEU. The materials used for cladding include zirconium, zircaloy and stainless steel. Successive fission cycles were run for determination of the criticality. **Table 2** shows the neutron absorption cross-sections and thermal conductivities for different clad materials at 25°C [12].

	Cr	Si	Mn	Fe	Ni	Mo	B	Sn	Zr	Zr-alloy	Steel
σ_a (barns)	3.1	0.17	13.3	2.56	4.49	2.6	750	0.63	0.184	0.22	3.1
k($Wm^{-1}K^{-1}$)	93.9	149.2	7.81	79.5	90.9	138	27.4	66.8	22.6	21.5	16

Table 2. Neutron absorption cross-sections and thermal conductivities for common clad materials at 25°C.

http://dx.doi.org/10.5772/62572

3. Results and discussion

3.1. Criticality calculation

The neutron absorption cross-sections show the ease with which a material absorbs thermal neutrons generated from fission in the reactor core. The lower the neutron absorption cross-section, the less permeable a material is to thermal neutrons. The thermal conductivity also shows how efficient a material is in conducting heat. Materials with higher thermal conductivities are more efficient conductors of heat than those with low thermal conductivities. **Table 3** shows K_{eff} values at the beginning and end of core life (BOL and EOL) as well as the corresponding standard deviations. The K_{eff} value used here is a result of the statistical combination of the three different estimates used by MCNP (absorption, collision and scattering). The major control cards used were the KCODE and the KSRC card.

From the neutron absorption cross-section in **Table 2**, the thermal neutron absorption of zirconium and zircaloy are much lower than that of stainless steel. This explains the good K_{eff} value obtained for zircaloy and zirconium clad fuels as compared to that of stainless steel. The absorptivity also explains the degree of neutron interaction with the clad material. For zirconium and zircaloy, little neutron is absorbed and hence these neutrons remain in the reactor core and are able to initiate further fission processes. This also makes zirconium very effective in preventing radioactive fission fragments from escaping the fuel into the coolant and contaminating it. Again, when UOX and CEU fuel grade materials were used, similar patterns of K_{eff} were obtained with zirconium and zircaloy showing greater results for K_{eff} as compared to stainless steel. Even though zirconium has a slightly lower neutron absorption cross-section and comparable thermal conductivity relative to zirconium alloy as shown in **Table 2**, K_{eff} results for zircaloy look slightly higher than that of zirconium. This observation may be due to enhanced alloy properties.

The zircaloy cladding used is zircaloy-4, which is similar in composition to zircaloy-2, but has reduced nickel and iron compositions. The reaction of zirconium with steam at high temperatures produces hydrogen gas by the reaction (Eq. 7):

$$Zr + 2H_2O \rightarrow ZrO_2 + 2H_2 \tag{7}$$

FUEL	CLAD	K_{eff} at BOL	K_{eff} at EOL
MOX	Stainless steel	1.09295 ± 0.00120	0.92315 ± 0.00087
	Zircaloy	1.15778 ± 0.00145	0.98630 ± 0.00098
	Zirconium	1.15624 ± 0.00129	0.98258 ± 0.00098
UOX	Stainless steel	0.90130 ± 0.00193	0.81205 ± 0.00212
	Zircaloy	0.95456 ± 0.00140	0.80834 ± 0.00077
	Zirconium	0.93740 ± 0.00236	0.80754 ± 0.00049

FUEL	CLAD	K_{eff} at BOL	K_{eff} at EOL
CEU	Stainless steel	0.91187 ± 0.00311	0.80920 ± 0.00097
	Zircaloy	0.97923 ± 0.00210	0.86789 ± 0.00105
	Zirconium	0.95529 ± 0.00232	0.84828 ± 0.00054

Table 3. K_{eff} values for different clad materials at the beginning and end of burnup steps for MOX, UOX and CEU fuel.

Oxidation of zirconium metal reduces the ductility and robustness of zirconium metal, and hence increases the probability for the escape of thermal neutrons from the core of the reactor [12]. This further reduces the effectiveness of zirconium for higher and prolonged fuel burnups. With respect to zirconium alloys, the hydrogen produced by oxidation of zirconium in steam diffuses into the alloy, causing the formation of zirconium hydrides. The hydrides formed are less dense and more brittle than the zirconium alloy and leads to the weakening of the clad material. This is especially the case in zirconium-2 alloy. The zirconium-4 alloy has a reduced composition of iron and no nickel composition; this reduces the hydride effect by reducing the tendency to pick up hydrogen. This characteristic of zircaloy-4 used improves its mechanical properties, reducing the probability of escape of thermal neutrons considerably, thus improving the overall K_{eff} value in the long term.

The thermal conductivities listed in **Table 2** reveal a higher value for zirconium and zircaloy, as compared to that of stainless steel. A high value means that heat can be quickly conducted away from the reactor core to the coolant. This prevents very high temperature buildup in the core leading to the melting of the fuel material or clad. The thermal conductivity of zirconium alloys, with thermal expansivity of nearly one-third that of stainless steel, is superior compared to that of stainless steel and other nuclear fuel storage materials. This also gives zirconium alloys superior dimensional stability at elevated temperatures. MCNP offers a number of statistical checks to assess the validity of a criticality calculation, which can be found in the MCNP user's manual [11]. These were found to be in good agreement with the output file when cross-checked.

3.2. Nuclear fuel reactivity

Reactivity is the degree of neutron multiplication in the reactor core. This parameter is directly related to the tendency of the reactor core to change power level. Also, control rods can be used to obtain a desired power level change or keep the power level constant by adjusting the reactivity when raised or lowered into the reactor core. Other factors which affect the reactivity include the density and temperature of the coolant or moderator and also the fuel temperature and density.

The reactivity for the three different fuel grades is calculated as a function of burnup, and the peak reactivity determined for each fuel grade is shown in **Table 4**. The reactivity is evaluated as (Eq. 8):

$$\rho = \frac{k - 1}{k} \tag{8}$$

where k is the effective multiplication factor and ρ is the reactivity.

The peak reactivity is the highest reactivity obtained as a function of burnup for each fuel grade. Another parameter, the gain, is the difference between the peak reactivity and the reactivity at BOL [13]. The gain is usually used in breeding reactors to characterize the affinity of the nuclear fuel for breeding reactivity. The gain is useful in breeder reactors to measure the fuels affinity to breed 239Pu; however, it is not a very good parameter for determining the neutronics performance of the fuel. One of the most important measures of fuel performance is the peak reactivity. Since the reactivity has a direct bearing on the power level, the higher the peak reactivity, the much higher the power output. The peak and gain reactivities of the three different fuel grades as burnup proceeds are indicated in **Table 4**. Usually, fuels with higher peak reactivities are found to have much lower gain. UOX has much higher peak reactivity, but records the lowest gain in reactivity.

Reactivity	UOX	MOX	CEU
PEAK	0.270	0.142	0.155
GAIN	0.119	0.124	0.142

Table 4. Reactivity parameters for the different fuel grades.

MOX has a much lower peak value relative to UOX, but records a much higher gain in reactivity. The same is seen for CEU. A look at the compositions of the three fuel grades reveals that 235U forms the main fissile material in both UOX and CEU. Depletion of 235U is known to reduce the reactivity. The buildup of actinides due to neutron absorption of 238U is also known to reduce the reactivity. These two factors occur in both UOX and CEU and might cause loss of reactivity, but this is compensated by the buildup of 239Pu and 241Pu in these two fuels. However, in MOX fuel, added to the depletion of 235U and 238U which reduces the reactivity, the reactivity is further reduced by the depletion of 239Pu and 241Pu, which are the main fissile materials in MOX fuel. This is seen in the relatively low peak value recorded for MOX fuel.

3.3. Burnup calculations

An expected core lifetime of 220 days is used for the reactor core since the K_{eff} drops drastically after this period, hence reducing the criticality. Usually, using large time steps of 50 and above leads to encountering large flux shape change and may lead to inaccurate results. Time steps small enough to capture the flux-shape change accurately over time is necessary according to Pelowitz [14]. Again, the time step chosen for a particular reaction depends on the core lifetime of the reactor with larger core lifetimes having larger time steps. Khattab et al. [7] used a 20-day time step for a 200 days expected operating life time of an MNSR. The 10-day period (between 60 and 70 days) was chosen to allow for maintenance operations. No burnup is

carried out within this period and the fuel may decay within this period from the heat built up in the core. The 10-day time step was chosen from examples used in the MCNPX user's manual [14].

In all, the uranium nuclide inventory shows similar variation with burnup time for all three different fuel grades. There is a rapid decrease of 235U and a slightly lower decrease for 238U in burnup time because these radionuclides are consumed as the fission process progresses. 236U radioisotopes, which are not fissile with thermal neutrons and are generated mainly due to gamma radiation emission of 235U as fission proceeds, are observed to increase with burnup time for each of the three fuel grades. Very little of 238U is consumed in the fission process as this is only fissionable and the main fissile material is 235U, which decreases rapidly. The uranium inventory is found to decrease for MOX fuel, but on a slightly lower scale relative to the other fuel grades due to relatively little uranium composition used in its fabrication. Our study shows that the 240Pu isotope is observed to buildup steadily for each of the three fuel grades. The 240Pu radioisotope, however, rises on a much higher scale in MOX than in CEU and UOX. This is because 240Pu is formed in a nuclear reactor by occasional neutron capture by 239Pu, much of which forms the initial fissile fuel material in MOX fuel.

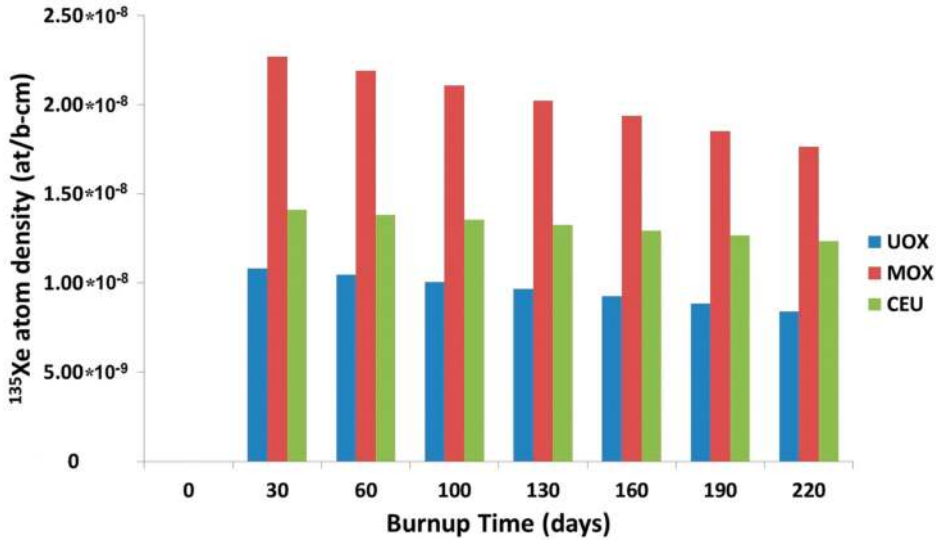

Figure 3. Atom density of 135Xe as a function of burnup time.

For 135Xe in **Figure 3**, a similar pattern is observed for all three fuel grades. There is a rapid accumulation of 135Xe after the first burn step, a result which might lead to a drastic drop in K_{eff}. This is known as the xenon poisoning. The production of 135Xe isotopes after this burn step gradually decreases, a result which helps to regulate the reactivity of the system. The accumulation of the fission product 135Cs shows a linear variation with the burnup time for all three fuel grades as seen in **Figure 4**.

http://dx.doi.org/10.5772/62572

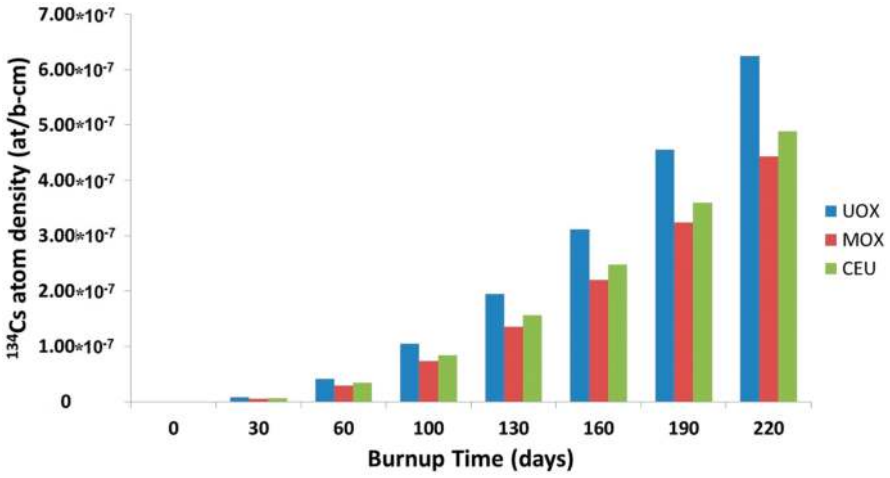

Figure 4. Atom density of 134Cs as a function of burnup time.

3.4. Time evolution of the K_{eff}

The study of the variation of K_{eff} with core burnup is of much importance as it describes whether or not the chain reaction in a nuclear reactor is stable or self-sustained. The results also give very important details on the core lifetime, defined as the length of time the reactor effective multiplication factor is above one. There is a large drop in K_{eff} during the first burn step as shown in **Figure 5**. This drop can be attributed to a drastic reduction in reactivity due primarily to the buildup of burnable poisons such as 135Xe and the depletion of fresh fuel. The K_{eff} is then gradually seen to decrease.

A similar pattern of the variation of K_{eff} with time is observed in all three different fuel grades. MOX fuel, however, might be much more effective in improving the core lifetime of the reactor, as K_{eff} is observed to remain critical for a much longer time relative to the other fuels. For UOX and CEU to maintain criticality for longer burn days, an increase in the mass fractions or weight percent (particularly for the fissile isotopes) is required. This is not too desirable due to the extremely high cost involved.

Hermine et al. [15] conducted research on the variation of K_{eff} with burnup time using AP1000 and a very high temperature reactor (VHTR) fuel cycle. Transuranic fuel arising from the AP1000 reactor was used as a part of fuel-loading of the VHTR. Transuranic fuels are fuels in which conventional uranium fuels have been mixed with a transuranic element (elements with atomic number greater than 92) in the form of mainly plutonium. A transuranic fuel containing 40% of weapons-grade plutonium (WGPu) was found as the best compromise [15]. A drastic first drop in K_{eff} occurred due to the depletion of burnable poisons, which is also observed in this study. The reactor life was extended by at least 36.7% when part of the low enriched uranium (LEU) is replaced by TRU, a result which agrees with the ability of TRU fuel to remain critical for a much longer time.

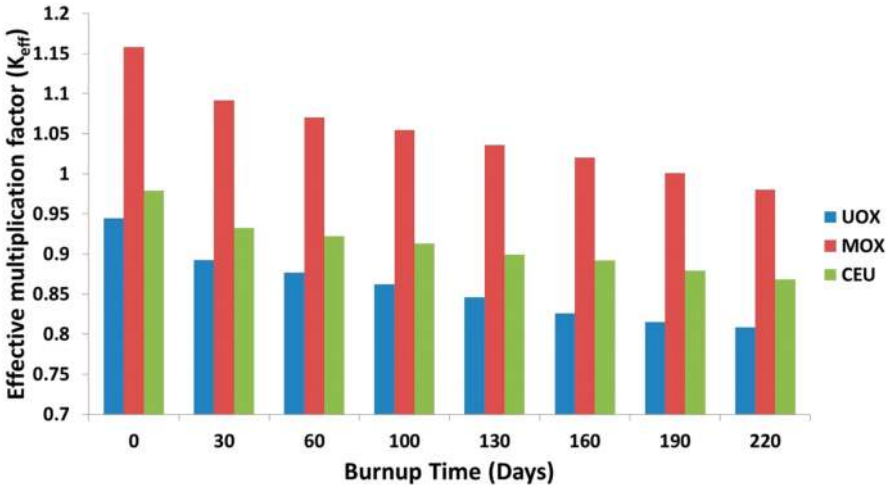

Figure 5. K_{eff} of different fuel grades as a function of burnup time.

The atom densities and radioactivities in Bequerel were calculated for each of the three fuel grades at the end of the 220-day burnup. The total radioactivities of both actinides and non-actinides were calculated for each fuel grade as shown in **Table 5**. In the event of a severe reactor core accident, the radiological hazard posed is proportional to the concentrations and radioactivities of these radionuclides. The total atom densities and radioactivities are also very important parameters in estimating which fuel grade performs better, posing a relatively less hazard at the end of the burnup time or core lifetime of the reactor. For the same burnup time, MOX fuel is found to have a relatively less total radioactivity of the reactor core, almost 15% reduction as compared to the other fuel grades.

The results from the burnup simulations were compared with some results obtained from literature to assess the validity. Yan Cao et al. [6] performed burnup simulations using the MCNPX code for a PWR with 3.15% enriched UO2 fuel. The uranium isotope depletion, increase in fissile plutonium isotope and that of 241Pu and 242Pu in that simulation are in good agreement with the results obtained from this study. Also, in assessing the accuracy of a new Monte Carlo based burnup code, burnup simulations were performed for a VVER-1000 assembly using UO2 and UO2GDO3 nuclear fuel types [5]. Again, the plot of atom densities of key radionuclides with burnup time showed good agreement with the results obtained from this study. Khattab et al. calculated the total radioactivity for a 220-day burnup period of a miniature neutron source reactor using the GETERA code. The total radioactivity at the end of the reactor core was calculated based on 19 selected radionuclides, which were considered essential to potential radiological hazard associated with the severe reactor accident in the MNSR core. This value was found to be 9.462×10^{13} Bq [7]. This study calculated the total radioactivities of the reactor core based on all radioactive actinides and non-actinides present at the end of the reactor core life as shown in **Table 5**. Comparison of the values shows reasonable agreement.

FUEL	Actinide activity (Bq)	Non-actinide activity (Bq)	Total activity (Bq)
UOX	1.6507×10^{19}	2.6011×10^{19}	4.25167×10^{19}
MOX	1.04663×10^{19}	2.59259×10^{19}	3.63859×10^{19}
CEU	1.94102×10^{19}	2.62367×10^{19}	4.56739×10^{19}

Table 5. Total activities of actinides and non-actinides after core burnup.

3.5. System Burnup and Neutronics Data

The burnup is given in units of gigawatt days (GWD) per metric tons of uranium (MTU), where MTU is the sum of the masses of isotopes with protons ≥90. The nuclear fission rate (f) is calculated from the product of the macroscopic fission cross-section ($\sum f$) and the neutron flux (). The power density (p) is determined as the product of the nuclear fission rate and the energy per fission (w). The average neutron flux is thus directly proportional to the power level in the reactor. As fuel consumption takes place with time, the neutron flux also increases, since the power is also directly related to the fuel content.

A look at the neutron fluxes of all three fuel grades reveals a general increase with time as seen in **Tables 5–7**, with UOX having a slightly higher average flux relative to CEU and MOX. The neutron flux increased by 20% for UOX fuel compared to a 17% increase in MOX fuel. The flux for UOX fuel at the end of burnup exceeds that of CEU by 17.87% and MOX by 22.68% with that of CEU exceeding MOX by 6%. This characteristic of UOX which may be due to its high fissile material density enhances the system power level. Again, these results agree with the peak reactivity parameter results in **Table 4** in which UOX and CEU had much higher reactivity relative to MOX. The burnup values indicate the fission energy released per metric ton of uranium. MOX fuel indicates comparable, but slightly higher, values of fuel burnup relative to UOX as shown in **Tables 6** and **7**. The burnup value at the end of the burn step for MOX exceeds that of CEU by 44% and UOX by 23%. This is due to the fact that MOX fuel remains much critical for a high part of the burnup period relative to the other two. **Table 8** shows CEU fuel with much lower fuel burnup values relative to the other two fuels, which may be due to its lower fissile material density.

Step	Time (days)	Flux (n/cm^2-s)	Burnup (GWD/MTU)
0	0	2.31×10^{14}	0
1	30	2.44×10^{14}	2.01
2	60	2.50×10^{14}	4.01
3	70	0	4.01
4	100	2.57×10^{14}	6.02
5	130	2.65×10^{14}	8.02
6	160	2.72×10^{14}	1.00

Step	Time (days)	Flux (n/cm²-s)	Burnup (GWD/MTU)
7	190	2.81×10^{14}	12.00
8	220	2.91×10^{14}	14.00

Table 6. Neutronics and burnup data for UOX fuel.

Step	Time (days)	Flux (n/cm²-s)	Burnup (GWD/MTU)
0	0	1.85×10^{14}	0
1	30	1.96×10^{14}	2.05
2	60	2.00×10^{14}	4.11
3	70	0	4.11
4	100	2.05×10^{14}	6.16
5	130	2.09×10^{14}	8.21
6	160	2.14×10^{14}	1.03
7	190	2.19×10^{14}	1.23
8	220	2.25×10^{14}	1.44

Table 7. Neutronics and burnup data for MOX fuel.

Step	Time (days)	Flux (n/cm²-s)	Burnup (GWD/MTU)
0	0	2.06×10^{14}	0
1	30	2.17×10^{14}	1.16
2	60	2.20×10^{14}	2.32
3	70	0	2.32
4	100	2.23×10^{14}	3.47
5	130	2.26×10^{14}	4.63
6	160	2.31×10^{14}	5.79
7	190	2.35×10^{14}	6.95
8	220	2.40×10^{14}	8.10

Table 8. Neutronics and burnup data for CEU fuel.

4. Conclusions

Parallel computing of fuel burnup in nuclear reactors give important insight about the chain reaction, the fuel consumption and buildup of radionuclides. The comprehensive calculations clearly present the characterization of the neutron flux, which is essential in the reactor design.

http://dx.doi.org/10.5772/62572

Fuel burnup is one of the most important reactor core parameters in the operation of nuclear reactors as well as any fuel research program. In this research, Monte Carlo burnup simulations of a critical pressurized water reactor system were carried out using three different fuel grades: MOX, UOX and CEU. The effect of different clad materials on K_{eff} was also analyzed.

The study of reactor neutronic parameters showed UOX fuel performs better relative to MOX and CEU. The peak reactivity of UOX was found to be 0.270 compared to 0.142 and 0.155 for MOX and CEU fuel, respectively. Also, the neutron flux for UOX exceeds that of CEU and MOX by 17.87 and 22.68%, respectively.

Zircaloy, with low thermal neutron absorption cross-section and high thermal conductivity produced better results for K_{eff} and hence proves to be a much more effective clad material.

The atom densities and radioactivities in Bequerel were calculated for each of the three fuel grades at the end of the 220-day burnup. The total atom densities and radioactivities of both actinides and non-actinides were calculated for each fuel grade. This was found to be 4.251e19Bq for UOX fuel and 3.639e19Bq and 4.567e19Bq for MOX and CEU fuel, respectively. In the event of a severe reactor accident, the radiological hazard posed is proportional to the concentrations and radioactivities of these radionuclides. The total atom densities and radioactivities are also very important parameters in estimating which fuel grade performs better in the sense of posing relatively few hazards at the end of the burnup time or core lifetime of the reactor. For the same burnup time, MOX fuel was found to have a relatively less total radioactivity of the reactor core, almost 15% reduction as compared to the other fuel grades.

Acknowledgements

This work is supported by the National Science Foundation (NSF) through the Center for Energy and Environmental Sustainability (CEES), a NSF CREST Center (Award NO. 1036593).

Author details

Raghava R. Kommalapati[1*], Fiifi Asah-Opoku[2], Hongbo Du[3] and Ziaul Huque[4]

*Address all correspondence to: rrkommalapati@pvamu.edu

1 Center for Energy & Environmental Sustainability and Department of Civil and Environmental Engineering, Prairie View A&M University, Prairie View, TX, USA

2 Center for Energy & Environmental Sustainability, Prairie View A&M University, Prairie View, TX, USA

3 Center for Energy & Environmental Sustainability, Prairie View A&M University, Prairie View, TX, USA

4 Department of Mechanical Engineering, and Center for Energy & Environmental Sustainability Prairie View A&M University, Prairie View, TX, USA

References

[1] Kim C.-S.; Kim C.-K.; Martin P.; Sansone U., Determination of Pu isotope concentrations and isotope ratio by inductively coupled plasma mass spectrometry: a review of analytical methodology. Journal of Analytical Atomic Spectrometry 2007, 22 (7), 827–841. DOI: 10.1039/b617568f.

[2] Alonso J.I.G.; Sena F.; Arbore P.; Betti M.; Koch L., Determination of fission products and actinides in spent nuclear fuels by isotope dilution ion chromatography inductively coupled plasma mass spectrometry. Journal of Analytical Atomic Spectrometry 1995, 10, 13. DOI: 10.1039/JA9951000381.

[3] Nicolaou G., Provenance of unknown plutonium material. Journal of Environmental Radioactivity 2008, 99 (10), 1708–1710. DOI: 10.1016/j.jenvrad.2008.06.001.

[4] Joe K.; Jeon Y.-S.; Han S.-H.; Lee C.-H.; Ha Y.-K.; Song K., Determination of plutonium content in high burnup pressurized water reactor fuel samples and its use for isotope correlations for isotopic composition of plutonium. Applied Radiation and Isotopes 2012, 70 (6), 931–936. DOI: 10.1016/j.apradiso.2012.03.015.

[5] El Bakkari B.; ElBardouni T.; Nacir B.; ElYounoussi C.; Boulaich Y.; Meroun O.; Zoubair M.; Chakir E., Accuracy assessment of a new Monte Carlo based burnup computer code. Annals of Nuclear Energy 2012, 45, 29–36. DOI: 10.1016/j.anucene.2012.02.011.

[6] Cao Y.; Gohar Y.; Broeders C.H.M., MCNPX Monte Carlo burnup simulations of the isotope correlation experiments in the NPP Obrigheim. Annals of Nuclear Energy 2010, 37 (10), 1321–1328. DOI: 10.1016/j.anucene.2010.05.015.

[7] Khattab K.; Dawahra S., Calculation of fuel burnup and radionuclide inventory in the Syrian miniature neutron source reactor using the GETERA code. Annals of Nuclear Energy 2011, 38 (6), 1442–1446. DOI: 10.1016/j.anucene.2011.01.030.

[8] Chadwick M.B.; Young P.G.; Chiba S.; Frankle S.C.; Hale G.M.; Hughes H.G.; et al. Cross-section evaluations to 150 MeV for accelerator-driven systems and implementation in MCNPX. Nuclear Science and Engineering 1999, 131 (3), 293–328. DOI: 10.13182/NSE98-48.

[9] Filges D.; Goldenbaum F.; Enke M.; Galin J.; Herbach C.M.; Hilscher D.; et al. Spallation neutron production and the current intra-nuclear cascade and transport codes. European Physical Journal A. 2001, 11 (4), 467–490. DOI: 10.1007/s100500170058.

[10] U.S. Nuclear Regulatory Commission, "Fault Tree Handbook", NUREG-0492. Available from: http://www.nrc.gov/reading-rm/doc-collections/nuregs/staff/sr0492/ [Accessed 15 December 2015].

[11] Brown F.; Kiedrowski B.; Bull J., "MCNP 1.60 release notes", Los Alamos National Laboratory, LA-UR-10-06235. 2008. Available from: https://laws.lanl.gov/vhosts/mcnp.lanl.gov/pdf_files/la-ur-10-06235.pdf [Accessed 20 December 2015].

[12] Asah-Opoku F.; Liang Z.; Huque Z.; Kommalapati R.R., Burnup simulations of different fuel grades using the MCNPX Monte Carlo Code. Nuclear Technology & Radiation Protection 2014, 29 (4), 259–267. DOI: 10.2298/ntrp1404259a.

[13] Yarsky P. Core design and reactor physics of a breed and burn gas-cooled fast reactor [Thesis], 2005. Pages 74–76, Massachusetts Institute of Technology. Cambridge, MA, USA.

[14] Pelowitz D.B., MCNPX user's manual version 2.7.0. LA-CP-11-00438. Los Alamos National Laboratory. 2011.

[15] Cuvelier M.-H.M.; Tsvetkov P.V., TRU management and U-235 consumption minimization in fuel cycle scenarios with AP1000 and VHTRs. Annals of Nuclear Energy 2013, 55, 137–150. DOI: 10.1016/j.anucene.2012.11.015.